PROCEEDINGS OF SCIENCE

Search for low-scale gravity signatures in multi-jet final states with the ATLAS detector at $\sqrt{s}$ = 8 TeV

Kuhan Wang[*1] **and Patrick Czodrowski**[2]
On behalf of the ATLAS Collaboration
1. *McGill University*
2. *University of Alberta*
e-mail: kwang@cern.ch, czodrows@cern.ch

A search for physics beyond the Standard Model in the multi-jet final state using 20.3 fb^{-1} of $\sqrt{s}$ = 8 TeV pp collision data recorded in 2012 using the ATLAS detector at the LHC is presented. The observed data is statistically compatible with the background prediction. The results are interpreted in terms of upper limits on the visible cross section for non-SM production of multi-jet final states at the 95% confidence level. In addition, using a number of models of low-scale gravity, exclusion contours are drawn in the space of lower-mass threshold of production and fundamental Planck/string mass. These contours exclude the lower-mass threshold for black hole and string ball production ranging from 4.6 to 6.2 TeV.

The European Physical Society Conference on High Energy Physics
22–29 July 2015
Vienna, Austria

[*]Speaker.

PoS(EPS-HEP2015)151

1. Introduction and background

A search for physics beyond the Standard Model in the multi-jet final state using 20.3 fb^{-1} of $\sqrt{s} = 8$ TeV pp collision data recorded in 2012 using the ATLAS detector [1] at the LHC is presented [2]. The observed data is statistically compatible with the background prediction. Extra spatial dimensions represent an extension to the current knowledge of fundamental physics [3], [4]. In theoretical models within the framework of extra spatial dimensions there exists the possibility that the fundamental Planck energy scale can be suppressed to order $\sim$TeV by factors related to the geometry and number (n) of extra dimensions. These predictions lead to the result that non-perturbative gravity could be accessible at hadron colliders in the form of the production of microscopic black holes, string balls and additional exotic objects. These black holes (string balls) are theorized to decay semi-classically into a thermal distribution of particles governed by the Hawking (Hagedorn) temperature. Due to the density of states, the relative emission by particle type will be dominated by hadronic contributions [5]. The characteristic final state signature is a large multiplicity of high transverse momentum, p_{T}, jets.

2. Event variables and data selection

In this analysis the event variables,

$$H_{\mathrm{T}} = \sum_{N_{\mathrm{Jet}}} p_{\mathrm{T}}, \tag{2.1}$$

representing the scalar sum (H_{T}) of the p_{T} of the total number (N_{Jet}) of jets in the event are used to isolate the signal against the Standard Model (SM) background and perform the analysis. Jets are defined as energy clusters reconstructed using the anti-k_t algorithm [6] with a cone radius of 0.4 within the kinematic constraints of $p_{\mathrm{T}} > 50$ GeV and pseudorapidity, $|\eta|, < 2.8$. A high H_{T} (> 700 GeV) trigger is used to select candidate events with at least one primary vertex and two associated tracks. Additional veto remove events recorded during non-optimal operating periods of the detector and energy deposition in non-functioning or mis-calibrated parts of the detector.

3. Monte Carlo simulation

Monte Carlo (MC) simulation is used to estimate the relative magnitudes of different SM contributions to the overall background and model and extract the systematic uncertainty effects of signal processes. Figure 1 compares the dominant SM processes given by MC simulation with data for two selected inclusive jet multiplicities ($N_{\mathrm{Jet}} \geq X$).

4. Analysis strategy

The analysis is conducted in the two dimensional space of H_{T} and $N_{\mathrm{Jet}} \geq X$. For each N_{Jet} slice the H_{T} distribution is divided into control (CR) and signal region (SR) based on kinematic considerations and signal contamination studies. low H_{T} range is defined to be the CR, free of evidence of new physics. An ansatz function,

$$\frac{dN}{dx} = p_0 \frac{(1-x)^{p_1}}{x^{p_2}}, \; x = \frac{H_{\mathrm{T}}}{\sqrt{s}}, \tag{4.1}$$

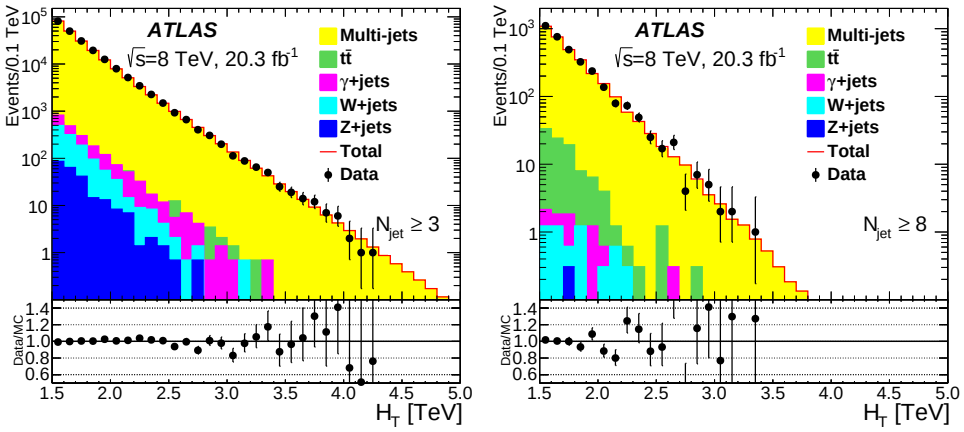

Figure 1: The H_{T} distribution for the $N_{\mathrm{Jet}} \geq 3$ (left) and $N_{\mathrm{Jet}} \geq 8$ (right) bins with data (black points) overlaid on top of MC simulation (colored histograms). [2]

is defined. A likelihood fit on the CR is used to fix the free parameters, p_0, p_1, p_2 of equation (4.1) and the function is extrapolated in x into the SR. The extrapolation is the central value of the background estimate and the analysis is repeated for each bin between $N_{\mathrm{Jet}} \geq 3$ to $N_{\mathrm{Jet}} \geq 8$. The range within which the function is fitted is found by considering the extrapolation of an ensemble of possible ranges and minimizing the difference in the background prediction between neighboring choices. The eight nearest neighbors of the nominal choice (1.5–2.9 TeV) is used to band the background estimate as a systematic uncertainty on the fitting range. The choice of the ansatz function, equation (4.1) is considered against a number of alternate functional forms that can be fitted to the CR to within a reasonable goodness of fit. A select number of these functions are illustrated in Figure 2 for the $N_{\mathrm{Jet}} \geq 3$ and $N_{\mathrm{Jet}} \geq 8$ bins. The maximum envelope with respect to the nominal choice (4.1) is assigned as the systematic uncertainty on the ansatz function choice.

5. Results and physical interpretations

The unblinded data is shown against the background estimate according to the method discussed in the previous section in Figure 3. The uncertainties associated with the fitting range, ansatz function choice and limited statistics are combined linearly to account for correlations. Search is conducted on the unblinded data in each SR to quantitatively measure the degree of data excess against the background. No statistically significant excesses are found and the H_{T} Variable is inclusively re-binned into $H_{\mathrm{T}}^{\mathrm{min}}$ as black hole events appear as a deviation in the tail of the H_{T} distribution. The $H_{\mathrm{T}}^{\mathrm{min}}$ of a particular bin is calculated by integrating the functions corresponding to the background estimate and each systematic uncertainty from the bin to the kinematic limit, $x = 1$. In the absence of new physics, model-independent upper limits on non-SM multi-jet production are placed at the 95% confidence level. The results are shown in Figure 4 for the bins $N_{\mathrm{Jet}} \geq 3$ and $N_{\mathrm{Jet}} \geq 8$. The visible limits are defined as $\sigma \times A \times \varepsilon$. The reconstruction efficiency ε is extracted from a variety of `CHARYBDIS2` [7] and `BlackMax` [8] simulated signal models. The signal efficiency is found to be $\sim 88\%$ with a root mean square

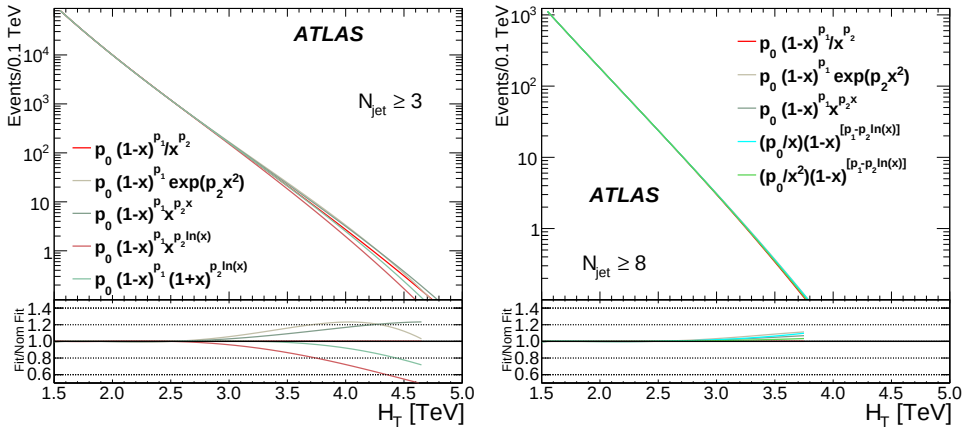

Figure 2: The H_{T} as described by various ansatz functions fitted to the CR ($1.5 < H_{\mathrm{T}} < 2.9$ TeV) and their extrapolations for the $N_{\mathrm{Jet}} \geq 3$ bin (left) and $N_{\mathrm{Jet}} \geq 8$ bin (right). The nominal choice is shown in red. [2]

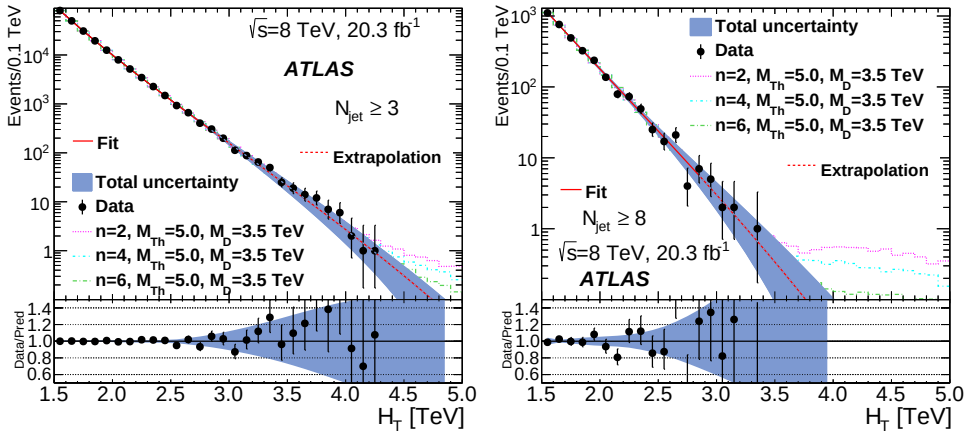

Figure 3: The H_{T} distributions, showing the data and extrapolated fits from the control region $1.5 < H_{\mathrm{T}} < 2.9$ TeV into the signal region $H_{\mathrm{T}} > 3.0$ TeV for the bins $N_{\mathrm{Jet}} \geq 3$ (left) and $N_{\mathrm{Jet}} \geq 8$ (right) and the combined uncertainty of the background prediction. Also shown are the expected black hole signals for three parameter sets of a non-rotating black hole model. [2]

(RMS) of $\sim 4\%$. The variation in ε between models is $\sim 1\%$ with a RMS of $\sim 1\%$. Therefore, the fiducial upper limit on non-SM multi-jet production can be placed as low as $\sigma \times A \sim 0.16$ fb. Furthermore, MC simulated signal samples are used to set model-dependent limits on select models of black hole and string ball production. The effects of jet energy scale, jet energy resolution and limited MC statistics are extracted from the simulation samples and further constrain the cross section limit. In Figure 5 the model-dependent limits for select models of black hole and string ball production are shown as exclusion contours in the space of lower-mass threshold of production, M_{th}, and fundamental Planck/string mass, $M_{\mathrm{D/s}}$. Generally, the exclusion power improves as a function of dimensionality due to increasing cross sections. As $M_{\mathrm{th}} \to M_{\mathrm{D/s}}$, the cross section decreases and the assumptions of semi-classical evaporation become less valid.

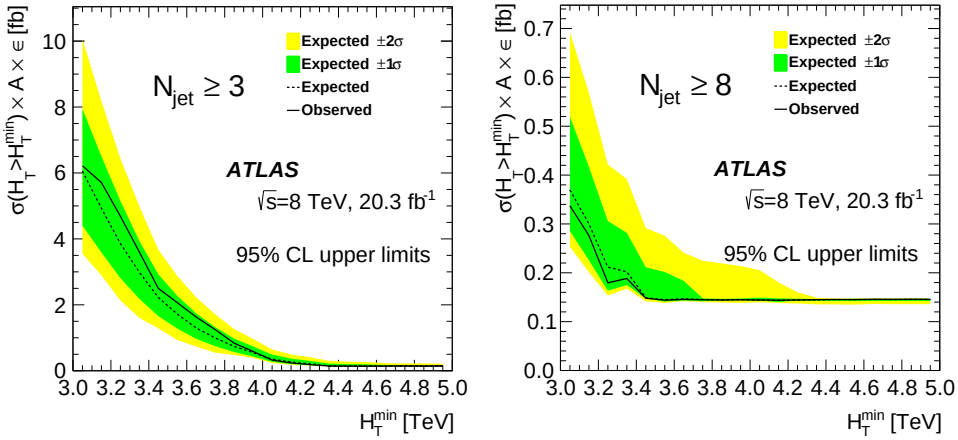

Figure 4: Model-independent upper limits on non-SM multi-jet production in $H_{\mathrm{T}}^{\mathrm{min}}$. for the bins $N_{\mathrm{Jet}} \geq 3$ (left) and $N_{\mathrm{Jet}} \geq 8$ (right). The dashed and solid black lines show the expected and observed limits, the green and yellow bands illustrate the one and two standard deviations on the expected limits. [2]

6. Summary

Search for beyond the SM physics in the multi-jet channel was conducted using 20.3 fb^{-1} of pp collision data recorded at $\sqrt{s}$ = 8 TeV. No evidence of new physics is found and the null results are interpreted in the context of a low-scale gravity search. Model independent fiducial upper limits are placed as low as 0.16 fb for events with $H_{\mathrm{T}}^{\mathrm{min}} > 4.3$ TeV. In addition, model dependent results exclude a wide variety of models of black hole and string ball production with $n = 2, 4, 6$ extra spatial dimensions for M_{th} values between 4.6 and 6.2 TeV. These results compare favorably with the analogous CMS search [9] and similar ATLAS results in the single lepton and jets [10] and dimuon final states [11].

References

[1] ATLAS Collaboration. The ATLAS Experiment at the CERN Large Hadron Collider. *JINST*, 03:S08003–00, 2008.

[2] ATLAS Collaboration. Search for low-scale gravity signatures in multi-jet final states with the ATLAS detector at $\sqrt{s} = 8$ TeV. *JHEP*, 07:032, 2015.

[3] N. Arkani-Hamed, S. Dimopoulos, and G. R. Dvali. The Hierarchy problem and new dimensions at a millimeter. *Phys. Lett.*, B429:263–272, 1998.

[4] I. Antoniadis, N. Arkani-Hamed, S. Dimopoulos, and G. R. Dvali. New dimensions at a millimeter to a Fermi and superstrings at a TeV. *Phys. Lett.*, B436:257–263, 1998.

[5] S. B. Giddings and S. D. Thomas. High-energy colliders as black hole factories: The End of short distance physics. *Phys. Rev.*, D65:056010, 2002.

[6] M. Cacciari, G. P. Salam, and G. Soyez. The Anti-k(t) jet clustering algorithm. *JHEP*, 04:063, 2008.

[7] C. M. Harris, P. Richardson, and B. R. Webber. CHARYBDIS: A Black Hole Event Generator. *JHEP*, 08:033, 2003.

[8] D. Dai, G. Starkman, D. Stojkovic, C. Issever, E. Rizvi, and J. Tseng. BlackMax: A black-hole event generator with rotation, recoil, split branes, and brane tension. *Phys. Rev.*, D77:076007, 2008.

[9] CMS Collaboration. Search for microscopic black holes in pp collisions at $\sqrt{s} = 8$ TeV. *JHEP*, 07:178, 2013.

[10] ATLAS Collaboration. Search for microscopic black holes and string balls in final states with leptons and jets with the ATLAS detector at $\sqrt{s} = 8$ TeV. *JHEP*, 08:103, 2014.

[11] ATLAS Collaboration. Search for microscopic black holes in a like-sign dimuon final state using large track multiplicity with the ATLAS detector. *Phys. Rev.*, D88(7):072001, 2013.

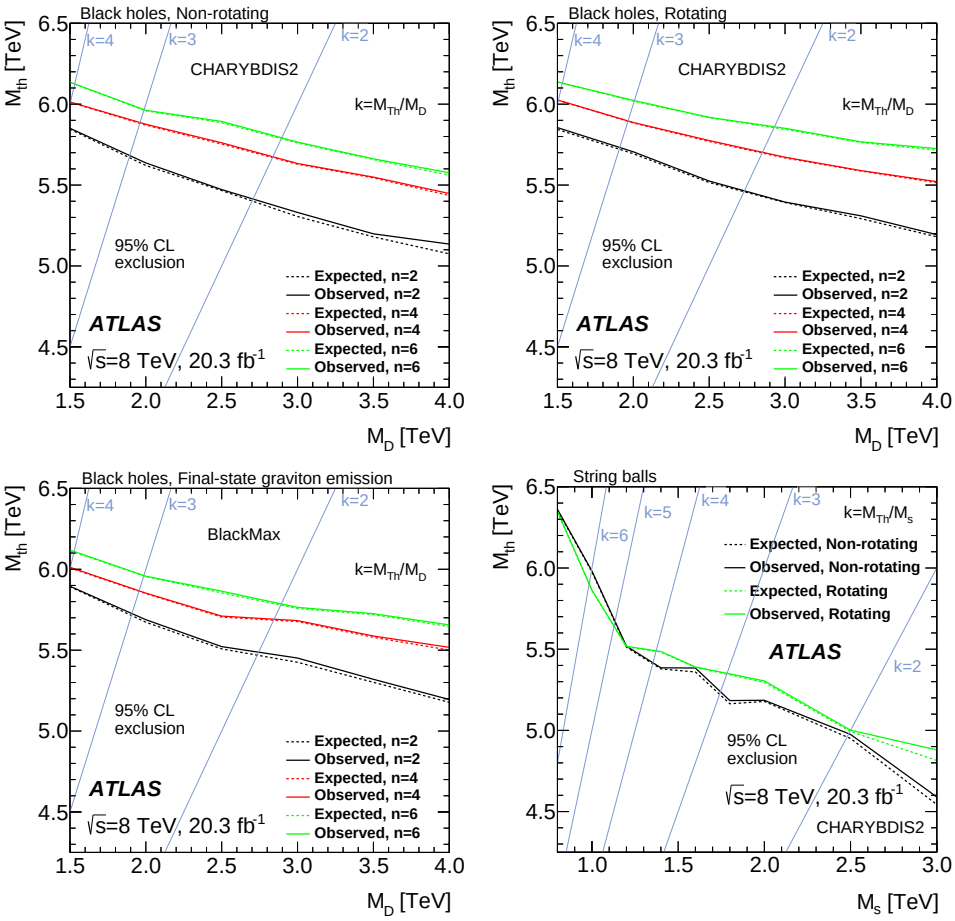

Figure 5: Model-dependent exclusion contours for non-rotating black holes (top left), rotating black holes (top right), black holes with final-state graviton emission (bottom left) and rotating and non-rotating string balls (bottom right). Differing number of extra spatial dimensions are grouped together for similar models. One and two standard deviation expected limit bands have been suppressed for clarity. Lines of constant $k = M_{\mathrm{th}}/M_{\mathrm{D/s}}$ define the relative validity of the model. [2]